THE JOURNAL OF BIOLOGICAL CHEMISTRY VOL. 282, NO. 40, pp. 29448–29456, October 5, 2007


# Mapping the Interacting Domains of STIM1 and Orai1 in $Ca^{2+}$ Release-activated $Ca^{2+}$ Channel Activation*[S]

Received for publication, April 30, 2007, and in revised form, August 10, 2007 Published, JBC Papers in Press, August 16, 2007, DOI 10.1074/jbc.M703573200

**Zhengzheng Li**[1], **Jingze Lu**[1], **Pingyong Xu**[1], **Xiangyang Xie, Liangyi Chen**[2], **and Tao Xu**[3]

*From the National Key Laboratory of Biomacromolecules, Institute of Biophysics, Chinese Academy of Sciences, Datun Road 15, Chaoyang District, Beijing 100101, China*

**STIM1 and Orai1 are essential components of $Ca^{2+}$ release-activated $Ca^{2+}$ channels (CRACs). After endoplasmic reticulum $Ca^{2+}$ store depletion, STIM1 in the endoplasmic reticulum aggregates and migrates toward the cell periphery to co-localize with Orai1 on the opposing plasma membrane. Little is known about the roles of different domains of STIM1 and Orai1 in protein clustering, migration, interaction, and, ultimately, opening CRAC channels. Here we demonstrate that the coiled-coil domain in the C terminus of STIM1 is crucial for its aggregation. Amino acids 425–671 of STIM1, which contain a serine-proline-rich region, are important for the correct targeting of the STIM1 cluster to the cell periphery after calcium store depletion. The polycationic region in the C-terminal tail of STIM1 also helps STIM1 targeting but is not essential for CRAC channel activation. The cytoplasmic C terminus but not the N terminus of Orai1 is required for its interaction with STIM1. We further identify a highly conserved region in the N terminus of Orai1 (amino acids 74–90) that is necessary for CRAC channel opening. Finally, we show that the transmembrane domain of Orai1 participates in Orai1-Orai1 interactions.**

$Ca^{2+}$ has been long recognized as an important second messenger in regulating a variety of physiological processes (1). In both excitable and non-excitable cells, it has been found that extracellular $Ca^{2+}$ enters the cytosol in a typical pathway after depletion of the endoplasmic reticulum (ER)[4] $Ca^{2+}$ store (2), which is therefore termed either capacitative calcium entry (3) or store-operated $Ca^{2+}$ (SOC) entry (4). The electrophysiological characteristics of this $Ca^{2+}$ entry were studied in 1992 and termed $Ca^{2+}$ release-activated $Ca^{2+}$ current ($I_{CRAC}$) (5). The molecular identity and mechanism of SOC or $I_{CRAC}$ have remained a mystery for a long time. Recently, however, several different groups have identified STIM1 (6, 7) and Orai1 (8–10) to be essential components of the CRAC channel.

STIM1 protein contains multiple discrete regions, including an EF-hand and a sterile $\alpha$-motif domain (SAM) in the N terminus (11, 12). In addition to a transmembrane region, STIM1 also contains a coiled-coil domain, a serine-proline-rich region, and a lysine-rich region in the C terminus (13–15), as shown in Fig. 1. Data clearly indicate that the EF-hand domain in the N terminus of STIM acts as a sensor of $Ca^{2+}$ concentration in the ER (16, 17) and participates in the formation of STIM1 puncta (11). It has been proposed that the ezrin/radixin/moesin (ERM) domain in the C terminus, containing the coiled-coil domain mediates the selective binding of STIM1 to TRPC1 and the cationic lysine-rich region, is essential for the gating of the TRPC1 channel (13). However, the precise roles of these domains of STIM1 in the signaling cascade of $I_{CRAC}$ activation are not known. By truncating different domains from STIM1, we address this question in this study.

It is known that STIM1 and Orai1 functionally interact with each other, because overexpressing both proteins (either human or *Caenorhabditis elegans* homologues) greatly potentiates the $I_{CRAC}$ current in human embryonic kidney 293 (HEK293) cells (18–20). We and other groups have found that $Ca^{2+}$ store depletion induces ER STIM1 aggregation and migration toward the plasma membrane (16, 21, 22), which lead to co-localized clustering of Orai1 on the surface membrane (21, 27), implying a physical interaction between STIM1 and Orai1. Recently, Takahashi *et al.* (23) showed that the N terminus of murine Orai1 is essential for store-operated $Ca^{2+}$ entry and is postulated to serve as a binding site for the ERM domain of STIM1. In addition, Orai1 is found to exist both as dimers and oligomers *in vivo* (24, 25). However, the domains of Orai1 that account for the STIM1-Orai1 or Orai1-Orai1 interactions remain unknown. Here we explore this field by co-expressing different truncated forms of Orai1 and STIM1, observing their spatial co-localization, and recording reconstituted SOC $Ca^{2+}$ entry signal and $I_{CRAC}$ current.

## EXPERIMENTAL PROCEDURES

*Solutions and Chemicals*—For intracellular $Ca^{2+}$ concentration ($[Ca^{2+}]_i$) measurements, we used standard extracellular Ringer's solution containing the following (in mM): 145 NaCl, 4.5 KCl, 2 $CaCl_2$, 1 $MgCl_2$, 10 D-glucose, and 5 Hepes (pH 7.4, adjusted with NaOH). The $CaCl_2$ was replaced by 1 mM EGTA

* This work was supported by the National Science Foundation of China (Grants 30400157, 30670503, 30670504, 30470448, and 30630020) and by the Major State Basic Research Program of China (Grants 2004CB720000 and 2006CB705700). The costs of publication of this article were defrayed in part by the payment of page charges. This article must therefore be hereby marked "*advertisement*" in accordance with 18 U.S.C. Section 1734 solely to indicate this fact.

[S] The on-line version of this article (available at http://www.jbc.org) contains supplemental Figs. S1–S9.

[1] These authors contribute equally to this work.

[2] To whom correspondence may be addressed: Tel.: 86-10-6488-8524; Fax: 86-10-6487-1293; E-mail: chen_liangyi@yahoo.com.

[3] To whom correspondence may be addressed: Tel.: 86-10-6488-8469; Fax: 86-10-6486-7566; E-mail: xutao@ibp.ac.cn.

[4] The abbreviations used are: ER, endoplasmic reticulum; SOC, store-operated $Ca^{2+}$; CRAC, $Ca^{2+}$ release-activated $Ca^{2+}$ channel; SAM, sterile $\alpha$-motif domain; ERM, ezrin/radixin/moesin; BAPTA, 1,2-bis(2-aminophenoxy)ethane-*N*,*N*,*N*′,*N*′-tetraacetic acid tetrakis; TG, thapsigargin; EGFP, enhanced green fluorescent protein; TIRFM, total internal reflection fluorescence microscope.

and 2 mM $MgCl_2$ in $Ca^{2+}$-free Ringer's solution. In patch clamp experiments, the standard external solution contained the following (in mM): 145 NaCl, 4.5 KCl, 10 $CaCl_2$, 1 $MgCl_2$, 10 D-glucose, 10 mM tetraethylammonium and 5 Hepes (pH 7.4, adjusted with NaOH). The divalent-free solution contained (in mM): 145 NaCl, 4.5 KCl, 10 EDTA, 10 mM tetraethylammonium, and 5 Hepes (pH 7.4, adjusted with NaOH). The pipette solution contained (in mM): 140 cesium glutamate, 8 $MgCl_2$, 12 BAPTA, and 10 Hepes (pH 7.2, adjusted with CsOH).

Stock solutions of thapsigargin (TG) were prepared in $Me_2SO$ at a concentration of 2 mM. External solutions were applied using a gravity-driven perfusion system, and the local solution was completely exchanged in less than 2 s. Fura-2/AM was purchased from Invitrogen. Unless otherwise specified all reagents and chemicals were from Sigma-Aldrich.

*Plasmid Construction*—pHluorin-STIM1, STIM1-mOrange, Orai1-EGFP, and Orai1-mOrange were constructed as previously described (21). The pH-sensitive fluorescent protein pHluorin was inserted immediately downstream of the predicted signal peptide region of human STIM1 (NM_003156) to produce pHluorin-STIM1. STIM1 tagged with different fluorescent proteins at either terminus exhibited identical spatial distribution, and either chimeric protein reconstituted SOC $Ca^{2+}$ entry and large CRAC current when co-expressed with Orai1 (Figs. 3 and 5), indicating that they were functionally equivalent. To obtain the Orai1–3×FLAG construct, Oria1 cDNA (NM_032790) was amplified by PCR from human placenta cDNA library (Invitrogen), tagged with 3×FLAG, and ligated into a pcDNA3.1 Zeo(+) vector. STIM1-ΔN (Δ23–200), STIM1-ΔC1 (Δ233–685), ΔC2 (Δ425–685), and ΔC3 (Δ672–685) were amplified by PCR from pHluorin-STIM1 and re-ligated into a KpnI- and EcoRI-digested pHluorin-STIM1 vector. Orai1-ΔN (Δ1–90), Orai1-ΔN73 (Δ1–73), Orai1-ΔC (Δ267–301), and Orai1-DΔ (Δ1–90 and Δ267–301) were amplified by PCR and cloned into pEGFP-N1 plasmid, respectively. The N terminus of Orai1 (1–90) and pHluorin tagged transmembrane domain (266–288) of Sytaxin1A (Stx1A) were amplified from Orai1-EGFP and Stx1A-pHluorin, respectively (26), ligated together in-frame by PCR and inserted into an EcoRI- and XhoI-digested pcDNA3.1 Zeo(+) vector (Orai1-Nt-TM). Similarly, an EGFP fragment was amplified by PCR, fused in-frame with the transmembrane domain of Stx1A, and ligated in a pcDNA3.1 Zeo(+) vector (EGFP-TM). All nucleotide sequences of constructs were verified by sequencing.

*Cell Culture, Transfection, and Fluorescence Imaging*—HEK293 cells were cultured as described previously (21) and were transfected with Lipofectamine™ 2000 (Invitrogen) following the manufacturer's instruction. One day prior to the experiment, cells were transferred onto round poly-L-lysine-coated coverslips. Expression levels of pHluorin-tagged STIM1 vectors or EGFP-tagged Orai1 vectors were quantified as the averaged fluorescence intensities obtained from transfected HEK293 cells under wide field illumination, as summarized in supplemental Fig. S1.

For imaging experiments, transfected cells were viewed either under a confocal laser scanning microscope FV500 (Olympus Optical Co., Tokyo, Japan) with 60× oil objective lenses (numerical aperture (NA) = 1.40) or under total internal reflection fluorescence microscope (TIRFM) with 100× oil lenses (NA = 1.45). Detail information regarding the construction and application of confocal and TIRFM are described elsewhere (21). For confocal microscopy experiments, we only showed the middle focal plane throughout this report unless otherwise specified. All images were processed and analyzed using ImageJ (National Institutes of Health).

*Single Cell $[Ca^{2+}]_i$ Measurement*—Cells were preincubated with 6 μM fura-2/AM at room temperature for 30 min in standard Ringer's solution. $[Ca^{2+}]_i$ was measured by a dual-wavelength excitation (340/380 nm) photometry system on an inverted microscope (IX71, Olympus, Tokyo, Japan) equipped with polychromatic xenon light source (TILL photonics, Gräfeling, Germany). The emission was collected at 510 ± 5 nm with a photodiode controlled by the TILL photometry system and X-Chart extension of Pulse software (HEKA, Lambrecht, Germany). $[Ca^{2+}]_i$ was calculated from the background-corrected fluorescence ratio *R*. Calibration parameters of $R_{min}$ (0.145), $R_{max}$ (4.069), and $K_{eff}$ (3.900 μM) were determined previously (28) .

*Electrophysiology*—Patch clamp experiments were conducted at room temperature using standard whole cell recording configuration. High resolution current recordings were acquired using the EPC-10 (HEKA). After establishment of the whole cell configuration, voltage ramps of 50-ms duration, spanning a range of −100 to +100 mV, were delivered from a holding potential of 20 mV every 2 s over a period of 300–500 s. All voltages were corrected for a liquid-junction potential of 10 mV. Currents were filtered at 2.9 kHz and digitized at a rate of 20 kHz. Capacitive currents were determined and corrected before each voltage ramp. The amplitude of the current recorded at −80 mV was used to monitor the development of $I_{CRAC}$ current. The maximum CRAC currents at −100 mV were used for statistical analysis. For noise analysis, 300-ms sweeps were acquired at the rate of 20 kHz at a holding potential of −100 mV, followed by a 50-ms ramp from −100 to +100 mV. Data were filtered offline at 1 kHz. The mean current and variant were calculated from a 200-ms segment in each 300-ms sweep.

*Co-immunoprecipitation and Western Blotting*—For transfection-based co-immunoprecipitation assays, HEK293 cells were transfected with the indicated plasmids, lysed in 500 μl of lysis buffer (50 mM Tris at pH 8.0, 500 mM NaCl, 0.5% Nonidet P-40, 1 mM dithiothreitol, and protease inhibitor tablets from Sigma-Aldrich), and immunoprecipitated with anti-FLAG-agarose beads (Sigma-Aldrich) overnight at 4 °C. The beads were washed four times with the lysis buffer and eluted in SDS sample buffer. Proteins in the cell lysates or immunoprecipitated samples were separated by SDS-PAGE, followed by Western blotting with anti-FLAG or anti-GFP (Santa Cruz Biotechnology, Santa Cruz, CA) antibody according to the standard procedures.

*Data Analysis*—Unless noted otherwise, all current traces were corrected for leak currents. Data analysis was conducted using IGOR Pro 5.01 (Wavemetrics, Portland, OR). Averaged results were presented as the mean value ± S.E. with the number of experiments indicated. Statistical significance was evaluated using Student's *t* test. Asterisks denote statistical signifi-

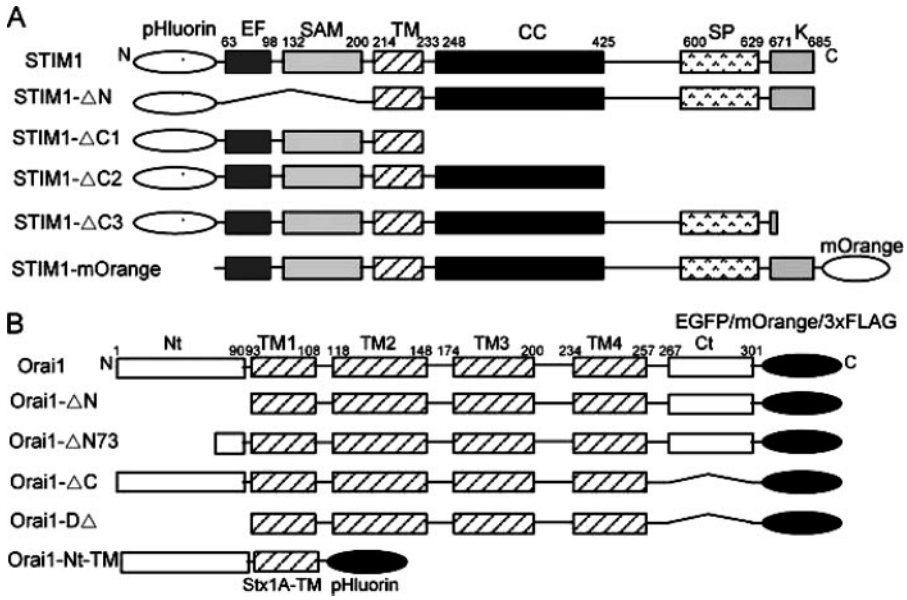


FIGURE 1. **A schematic representation of STIM1 (*A*) and Orai1 (*B*) mutants used in this study.** WT STIM1 and STIM1 mutants were fused with either pHluorin at the N terminus or mOrange at the C terminus. Functional domains of STIM1 include EF-hand, SAM, the transmembrane domain, coiled-coil (*CC*), the Ser/Pro-rich domain (*SP*), and the polylysine residues region (*K*). Orai1 includes four transmembrane domains with its N and C termini in the cytosol. Fluorescence tags (EGFP or mOrange) were fused to the C terminus of Orai1.

cance as compared with control, with a $p$ value less than 0.05 (*) and 0.01 (**).

## RESULTS

*Interrogations of Functions of Different Domains in STIM1*—To study the function of different domains of STIM1 in $Ca^{2+}$ store depletion-induced STIM1 aggregation and interaction with Orai1, we constructed different truncated forms of STIM1 and co-expressed them with wild-type (WT) Orai1. As shown in Fig. 1*A*, STIM1-ΔN was devoid of the EF hand and SAM domains in the N terminus but retained the signal peptide; STIM1-ΔC1 was lacking the entire cytosolic C terminus, whereas STIM1-ΔC2 lacked the serine-proline-rich region and the polycationic residue region. The STIM1-ΔC3 mutant was truncated such that it lacked most of the polycationic residues in the C terminus.

In accord with our previous data (21), WT pHluorin-STIM1 displayed diffused ER distribution in the resting state; it migrated toward cell periphery and co-localized with Orai1-mOrange on the plasma membrane after store depletion (supplemental Fig. S2). Deletion of the EF-hand and SAM domain in the N terminus of STIM1 led to a spontaneously targeting of STIM1 to the plasma membrane that was independent of store depletion, as shown in the confocal images obtained from the same cell before and after TG (1 $\mu$M) pretreatment for at least 5 min (Fig. 2*A*). Moreover, the fluorescence intensity profile of STIM1-ΔN and Orai1-mOrange along the line that was imposed across the cell overlapped, indicative of spatial co-localization of these proteins. Consistent with the optical experiment, cells co-expressing WT Orai1 and STIM1-ΔN exhibited a elevated basal $[Ca^{2+}]_i$ (supplemental Fig. S3*A*) and a spontaneously active inward current. The channel was blocked by 10 $\mu$M $La^{3+}$ (supplemental Fig. S3*C*) and had a current voltage relationship similar to native CRAC channel (supplemental Fig. S3*D*), indicating that it represented a *bona fide* CRAC channel. Expressing the pHluorin-tagged ΔC1 mutant in HEK293 cells resulted in a diffuse ER distribution, which failed to aggregate into clusters upon ER $Ca^{2+}$ store depletion (Fig. 2*B*). In contrast, STIM1-ΔC2 clusters were found in non-stimulated HEK293 cells, but many were not targeted to the cell periphery, as manifested by the fact that fluorescence intensity profile of STIM1-ΔC2 peaked in the cell interior in Fig. 2*C*. After store depletion, STIM1-ΔC2 clusters did not migrate to the surface membrane, neither did they co-localize with the WT Orai1 on the surface membrane. In parallel, SOC $Ca^{2+}$ influx was inhibited in cells co-expressing Orai1-mOrange with either STIM1 mutant (supplemental Fig. S3, *A* and *B*), and no CRAC current was detected in these cells, either (supplemental Fig. S8).

On the other hand, STIM1-ΔC3 exhibited normal ER distribution in rest condition; upon store depletion, they aggregated and migrated to the cell periphery and co-localized with Orai1-mOrange on the surface membrane, as shown by the overlapped fluorescence intensity profiles of the STIM1-ΔC3 and Orai1-mOrange along the lines that ran across the cell (Fig. 2*D*). Moreover, the STIM1-ΔC3 mutant was fully capable of reconstituting SOC influx when co-expressed with Oria1 in HEK293 cells (supplemental Fig. S3, *A* and *B*). Co-expressed STIM1-ΔC3 with Orai1 also produced large CRAC current (Fig. 3*A*). The I-V relationship of $I_{CRAC}$ current was not altered by expression of the STIM1-ΔC3 mutant (Fig. 3*B*), and the averaged current density was also similar in cells co-expressing STIM1-ΔC3 and Orai1-mOrange (30 ± 6 pA/picofarad, $n = 8$), as compared with cells co-expressing pHluorin-STIM1 and Orai1-mOrange (34 ± 5 pA/picofarad, $n = 8$). However, intracellular perfusion of BAPTA induced slower initiation of $I_{CRAC}$ current in cells co-expressing STIM1-ΔC3 and Orai1 (delay = 62 ± 11 s), as compared with cells co-expressing WT STIM1 and Orai1 (delay = 104 ± 23 s, $p < 0.05$) (Fig. 3*D*). This effect was not due to a difference in the exogenous fusion protein expressed, because overexpressed STIM1-ΔC3 and WT STIM1 were at a similar level (supplemental Fig. S1*A*). Taken together, these experiments indicate that different regions in STIM1 play different roles in clustering and migration of STIM and its functional interaction with Orai1 upon store depletion.

*Orai1 Interacts with STIM1 at Its Cytoplasmic C Terminus*—Orai1 is reported to functionally and physically interact with STIM1 and Orai1 (24, 25, 29). To locate sites in Orai1 that were responsible for this interaction, we truncated Orai1-EGFP of cytoplasmic C terminus (Orai1-ΔC), N terminus (Orai1-ΔN), and both

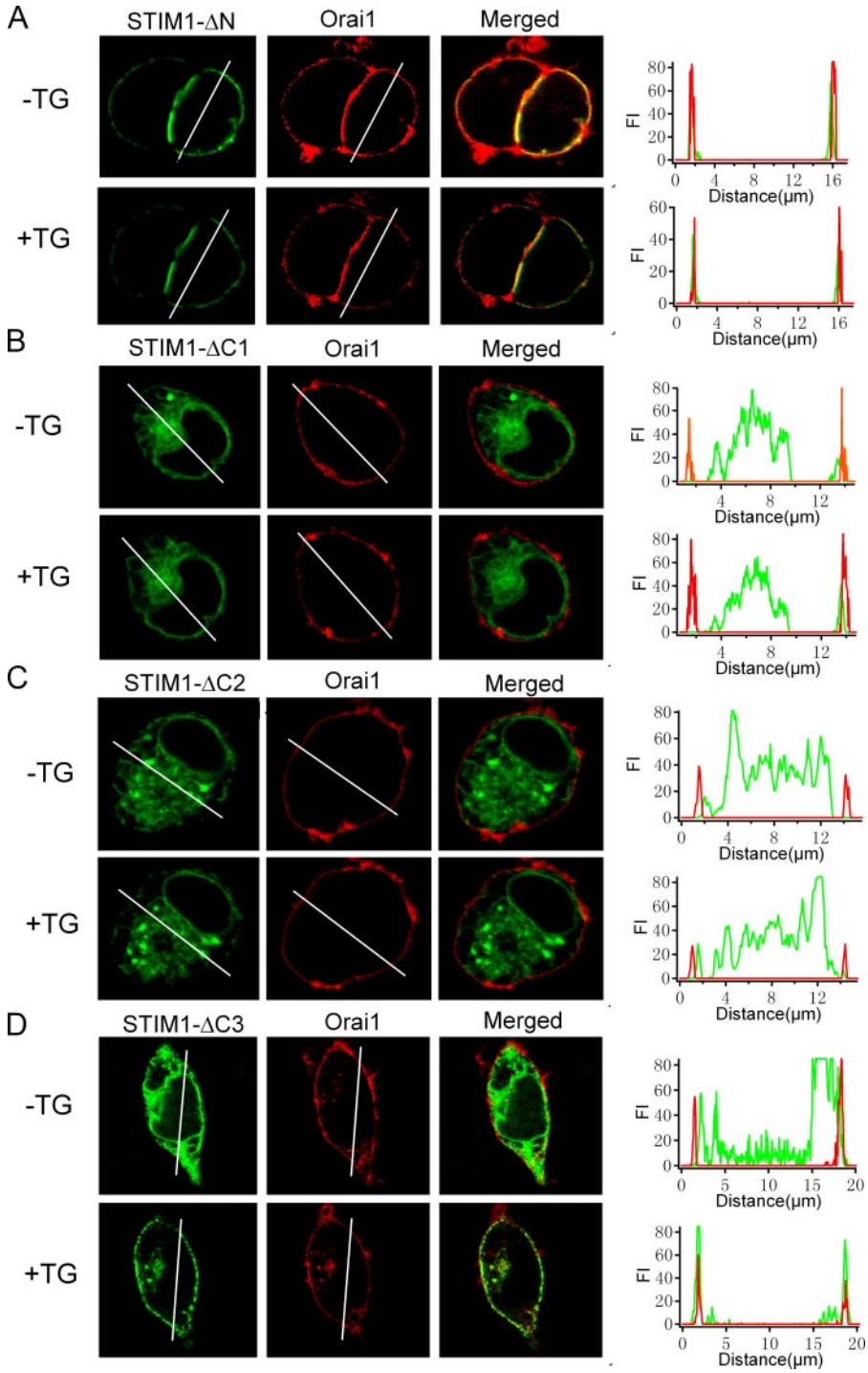


FIGURE 2. **Roles of different domains in STIM1 function.** Distribution of pHluorin-tagged STIM1 mutants lacking EF-hand and SAM domains (STIM1-ΔN, *A*) or whole cytoplasmic C terminus (STIM1-ΔC1, *B*), before and after TG stimulation (1 μM) in the same HEK293 cells. Images were captured at the middle plane using confocal microscopy. STIM1-ΔN was constitutively targeted to the plasma membrane, while STIM1-ΔC1 was unable to migrate to the cell periphery whether ER store was depleted or not. The *right panels* show spatial profiles of fluorescence intensity of STIM1 mutants (*green*) and Orai1-mOrange (*red*) along the *lines* imposed on the images. The *x axis* displays the distance relative to the start point of the *line*, and the *y axis* displays the fluorescence intensity (*FI*). *C*, deletion of the serine-proline-rich region and the polycationic residues region (STIM1-ΔC2) led to spontaneous STIM1 aggregations independent of $Ca^{2+}$ store depletion but was deficient in targeting to the plasma membrane. *D*, STIM1-ΔC3 exhibited normal ER distribution at rest and co-localized with Orai1-mOrange at the cell periphery after store depletion. Each set of images represents five similar experiments.

cytoplasmic C and N terminus (Orai1-DΔ). We also made a cytoplasmic N terminus of Orai1 fused to the trans-membrane domain of Syx1A tagged by pHluorin (Orai1-Nt-TM) (Fig. 1*B*). As a control, we have previously shown that overexpressed STIM1-mOrange in HEK293 cells aggregated into clusters that co-localized with Orai1-EGFP on the surface membrane after store depletion (21, 27). In contrast, as observed using TIRFM in Fig. 4*A*, Orai1-ΔC on the surface membrane failed to aggregate and co-localize with overexpressed STIM1-mOrange clusters after $Ca^{2+}$ store depletion by applying another sarcoplasmic-endoplasmic reticulum calcium ATPase pump blocker *tert*-butylhydroquinone (100 μM). Moreover, neither significant store-operated $Ca^{2+}$ entry (supplemental Fig. S4, *A* and *B*) nor CRAC current (supplemental Fig. S9) was observed in cells co-expressing Orai1-ΔC and STIM1-EGFP. In contrast, truncation of the cytoplasmic N terminus of Orai1 did not affect its cellular distribution, because Orai1-ΔN exhibited normal periphery distribution in rest conditions and co-localized with STIM1 clusters upon store depletion (Fig. 4*B*). Orai1-DΔ, where the double cytoplasmic region was removed, behaved similar to Orai1-ΔC when overexpressed with STIM1 (data not shown), implying that the cytoplasmic C terminus of Orai1 is crucial for its aggregation and co-localization with STIM1. This is further supported by the fact that overexpressed chimeric protein Orai1-Nt-TM, containing the cytoplasmic N terminus of Orai1, was targeted to the plasma membrane but failed to co-localize with STIM1 clusters after store depletion (Fig. 4*C*).

Although Orai1-ΔN responded to store depletion with the same spatial rearrangement as the WT Orai1, it failed to reconstitute either SOC $Ca^{2+}$ entry (supplemental Fig. S4, *A* and *B*) or CRAC current (supplemental Fig. S9) when co-expressed with STIM1, highlighting the essential role of cytoplasmic N terminus in CRAC channel opening.

*Amino Acids 74–90 in the Cytoplasmic N Terminus of Orai1 Are Required for CRAC Channel Activation*—By comparing the amino acid sequence of the human, mouse, *Drosophila*, and *C. elegans* Orai families (supplemental Fig. S5), we found that the

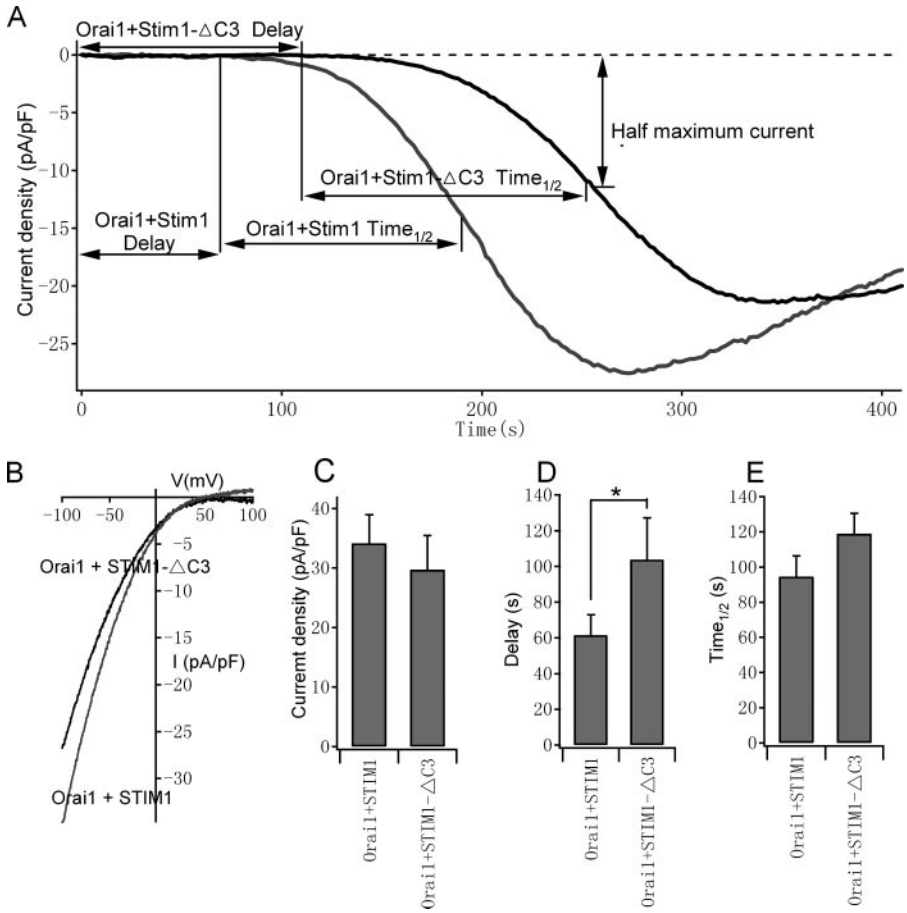


FIGURE 3. **Co-expression of Orai1-mOrange and STIM1-ΔC3 in HEK293 cells produce large CRAC current after ER store depletion.** *A*, current development evaluated at −80 mV in selected representative HEK293 cells expressing Orai1-mOrange plus pHluorin-STIM1 or Orai1-mOrange plus STIM1-ΔC3. Cells were bathed in external solution containing 10 mM $Ca^{2+}$ and dialyzed with 12 mM BAPTA-buffered internal solution to passively deplete stores. Whole cell recording configuration was achieved at time 0. Delay and $t_{1/2}$ are shown in the graph representing the time when the CRAC current was initiated and the time from the onset of CRAC current to 50% of maximum activation of the CRAC channel, respectively. *B*, leak-subtracted current-voltage relation of maximal CRAC current recorded in cells from *A*. *C*, summary of peak current densities at −100 mV in the indicated categories of cell ($n = 12$ for each group of cells). *D*, averaged delay of CRAC current development in HEK293 cells transfected with STIM1-ΔC3 plus Orai1-mOrange ($n = 12$) is significantly slower than averaged delay in cells transfected with pHluorin-STIM1 plus Orai1-mOrange ($n = 12$, $p < 0.05$). *E*, averaged $t_{1/2}$ in different cells.

amino acids from 74 to 90 in the cytoplasmic N terminus of Orai1 were highly conserved among different species. Therefore, we constructed a truncation sparing the conserved cytoplasmic N terminus (Orai1-ΔN73) (Fig. 1*B*). The amplitude of store-operated $Ca^{2+}$ entry was increased by 2-fold in HEK293 cells co-expressed with Orai1-ΔN73 and STIM1-mOrange (1.1 ± 0.12 μM, $n = 20$), compared with non-transfected cells (0.36 ± 0.05 μM, $n = 27$, $p < 0.001$), as shown in Fig. 5 (*A* and *B*).

Intracellular perfusion of high concentrations of BAPTA induced pronounced whole cell current in cells co-expressing Orai1-ΔN73 and STIM1-mOrange (Fig. 5*C*), which displayed similar CRAC channel characteristics such as an inwardly rectifying current-voltage relationship (Fig. 5*D*), an increase in divalent-free current in $Ca^{2+}$-free bath solution, and first potentiation then inhibition of the current by 50 μM 2-APB (supplemental Fig. S6). However, co-expressing Orai1-ΔN73 and STIM1-mOrange in HEK293 cells only reconstituted ~50% of the SOC $Ca^{2+}$ entry, and ~36% of $I_{CRAC}$ current compared with cells co-expressing STIM1-mOrange and Orai1-EGFP (Fig. 5, *C* and *E*). Such reduction of SOC $Ca^{2+}$ entry and CRAC current is not due to a decreased expression of Orai1-ΔN73 (supplemental Fig. S1*B*), and Orai1-ΔN73 exhibited normal plasma membrane localization similar to WT Orai1, as examined using TIRFM (data not shown). To further explore the underlying mechanism, we analyzed the variance and averages of whole cell current to infer characteristics of a single CRAC channel. In cells overexpressing STIM1 and Orai1, the variance of CRAC current *versus* its amplitude could be best fitted with a line with slope of 3.0 ± 0.2 fA (Fig. 5*G*), which represented single CRAC channel current multiplied by the result of 1 subtracted by the channel opening probability (30). This value was not different in cells co-transfected with Orai1-ΔN73 and STIM1 (3.0 ± 0.15 fA, Fig. 5*I*), indicating that single channel conductance might remain unaltered after truncating part of the N terminus of Orai1.

*Functional Interaction between Different Orai1*—Endogenous store-operated $Ca^{2+}$ entry was severely inhibited in HEK293 cells overexpressing WT Orai1 (70 ± 18 nM, $n = 22$) compared with non-transfected control cells (360 ± 53 nM, $n = 24$) (Fig. 6*A*), presumably reflecting a direct interaction of exogenous Orai1 with endogenous STIM1 or Orai1 that led to a functionally inactivated CRAC channel. Therefore, we probed possible interactions base on this criteria. Transfecting HEK293 cells with Orai1-ΔN was equally effective as WT Orai1 in reducing the amplitude of SOC $Ca^{2+}$ entry (88 ± 21 nM, $n = 21$, Fig. 6*B*). Although the inhibition was less pronounced compared with previous results, overexpressing Orai1-ΔC or Orai1-DΔ also significantly reduced the amplitude of endogenous SOC $Ca^{2+}$ entry (218 ± 26 nM, $n = 24$ and 118 ± 20 nM, $n = 24$ respectively) (Fig. 6*B*). It has been recently suggested that the N terminus of mouse Orai1 acts as a dominant negative mutant that inhibits SOC entry (23). Consistent with this idea, SOC $Ca^{2+}$ influx in cells expressing Orai1-Nt-TM was also significantly suppressed (160 ± 25 nM, $n = 21$).

Because Orai1-DΔ was incapable of forming clusters co-localized with STIM1, we wondered if Orai1-DΔ inhibited SOC influx through interacting with endogenous Orai1. To test that possibility, 3×FLAG-tagged WT Orai1 was co-expressed with either EGFP-tagged Orai1-DΔ or EGFP-tagged transmembrane domain of Syx1A (EGFP-TM). The two forms of Orai1

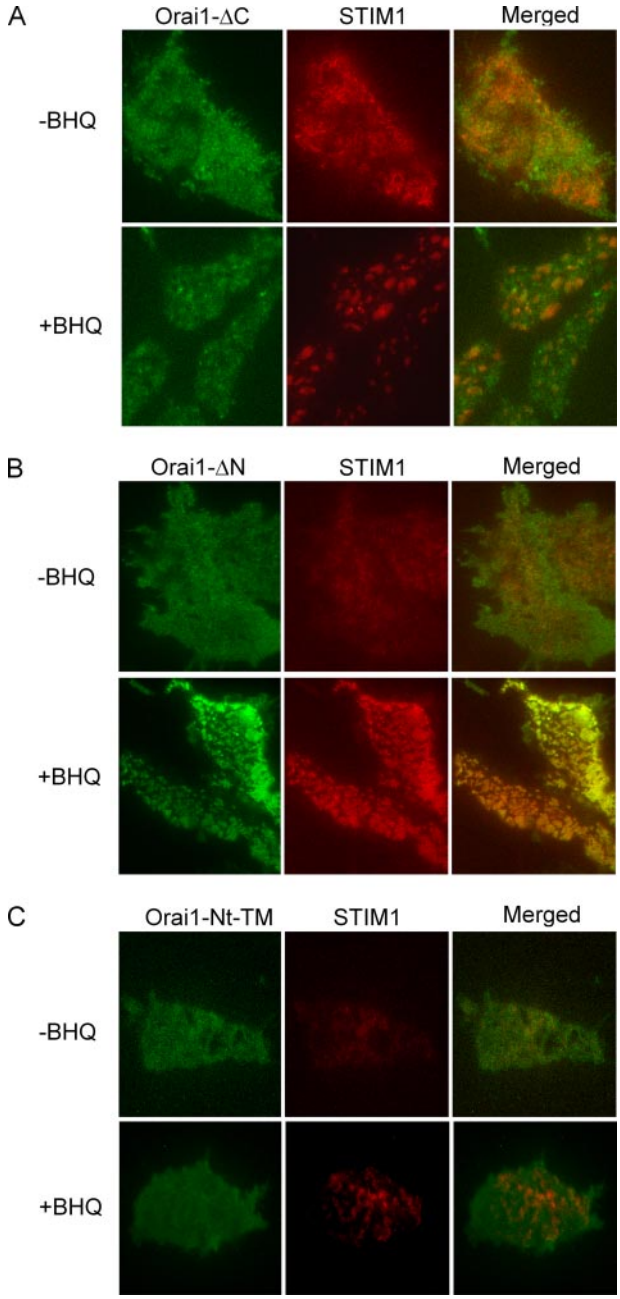


FIGURE 4. **The cytoplasmic C terminus of Orai1 is essential for its co-localization with STIM1.** TIRFM was used to examine distributions of EGFP-tagged Orai1 mutants and mOrange-tagged STIM1 mutants before or after store depletion. *A*, Orai1-ΔC was distributed throughout the surface membrane at rest (*upper left panel*). Depletion of the ER $Ca^{2+}$ store induced STIM1-mOrange aggregation into puncta underneath the plasma membrane, whereas Orai1-ΔC failed to co-localize with STIM1. As shown in the merged image (*right*), there is little overlap of Orai1 and STIM1 either before or after store depletion. *B*, Orai1-ΔN and STIM1-mOrange exhibited normal distribution at rest. After store depletion, Orai1-ΔN (*left*) and STIM1 (*right*) aggregated into co-localized clusters. *C*, Orai1-Nt-TM distributed homogenously throughout the surface membrane before and after store depletion and was incapable of forming clusters that co-localized with STIM1-mOrange. Each set of images represents at least five similar experiments.

interacted with one another, as shown by immunoblotting Orai1-DΔ-EGFP, which was co-immunoprecipitated with Orai1–3×FLAG (Fig. 6*C*). As a control, anti-FLAG beads failed to co-immunoprecipitate EGFP in control cells transfected with 3×FLAG-tagged Orai1 and EGFP-TM. These results indicate that the transmembrane domain of Orai1 is involved in the Orai1-Orai1 interaction.

## DISCUSSION

It is firmly established that STIM1 forms aggregates after ER $Ca^{2+}$ store depletion (6, 7, 21), which depends on the EF-hand and SAM domains in the N terminus of STIM1 (11, 16). In the present study, we further confirm this theory, because deletion of EF-hand and SAM domains leads to spontaneous plasma membrane targeting of STIM1 to the cell periphery and constitutive opening of the CRAC channel (Fig. 2 and supplemental Fig. S3). We also found that STIM1-ΔC1 was unable to form aggregates before or after store depletion, whereas STIM1-ΔC2 spontaneously aggregated into clusters in resting condition. The difference is likely to be the presence of the coiled-coil region, which is present in STIM1-ΔC2 but absent in the ΔC1 mutant, therefore strongly supporting an essential role for the coiled-coil domain in STIM1 aggregation (31). Huang *et al.* (13) reported that the ERM domain of STIM1 is essential for its binding with the TRPC1 channel, therefore suggesting a similar interaction between STIM1 and Orai1. In our study, $Ca^{2+}$ store depletion failed to induce STIM1-ΔC2 migration and Orai1 aggregation in cells co-expressing these two vectors, and this phenomenon was rescued by replacing STIM1-ΔC2 with STIM1-ΔC3. Because STIM1-ΔC3 vector contains a serine-proline-rich region and part of the ERM domain compared with the ΔC2 mutant (13), we further delineate these regions as possible STIM1-Orai1 interaction sites.

Human STIM1 has a polycationic tail, which is found to be essential for the gating of the TRPC1 channel (13). Many membrane-residing small GTPase proteins share a similar structure and use this polycationic tail to guide their targeting to the phosphatidylinositol 4,5-bisphosphate-enriched region in the plasma membrane (32). Therefore, it is tempting to speculate that this polycationic region determines the targeting of STIM1 to the cell surface. In agreement with this hypothesis, both TG-induced migration of STIM1-ΔC3 puncta to the cell periphery (data not shown) and development of $I_{CRAC}$ current induced by intracellular perfusion of BAPTA were slowed down, implying a reduced efficiency in the trafficking of STIM1 to the cell periphery. However, the amplitude of averaged $I_{CRAC}$ current reconstituted by STIM1-ΔC3 and Orai1 was not significantly different from that reconstituted by STIM1 and Orai1, indicating that the tail region is not required for CRAC activation. It is possible that the presence of the single basic amino acids in the tail region (amino acid 671) in our constructs, which was absent in previous studies (13), provides enough guiding signal for STIM1. However, Yeung *et al.* (33) showed that reducing the cationic residues in the K-*ras* tail down to two residues released it from plasma membrane subdomains, and at least four cationic residues in the tail were required for obvious binding of the protein to the cell periphery. Moreover, this polycationic region is not conserved in *C. elegans* or *Drosophila* (34). However, co-expressing STIM1 and Orai1 from *C. elegans* reconstitutes large $I_{CRAC}$ current in HEK293 cells (20). Therefore, we favor the concept that the highly conserved serine-proline-rich region serves as a ubiquitous targeting signal of STIM1, and the

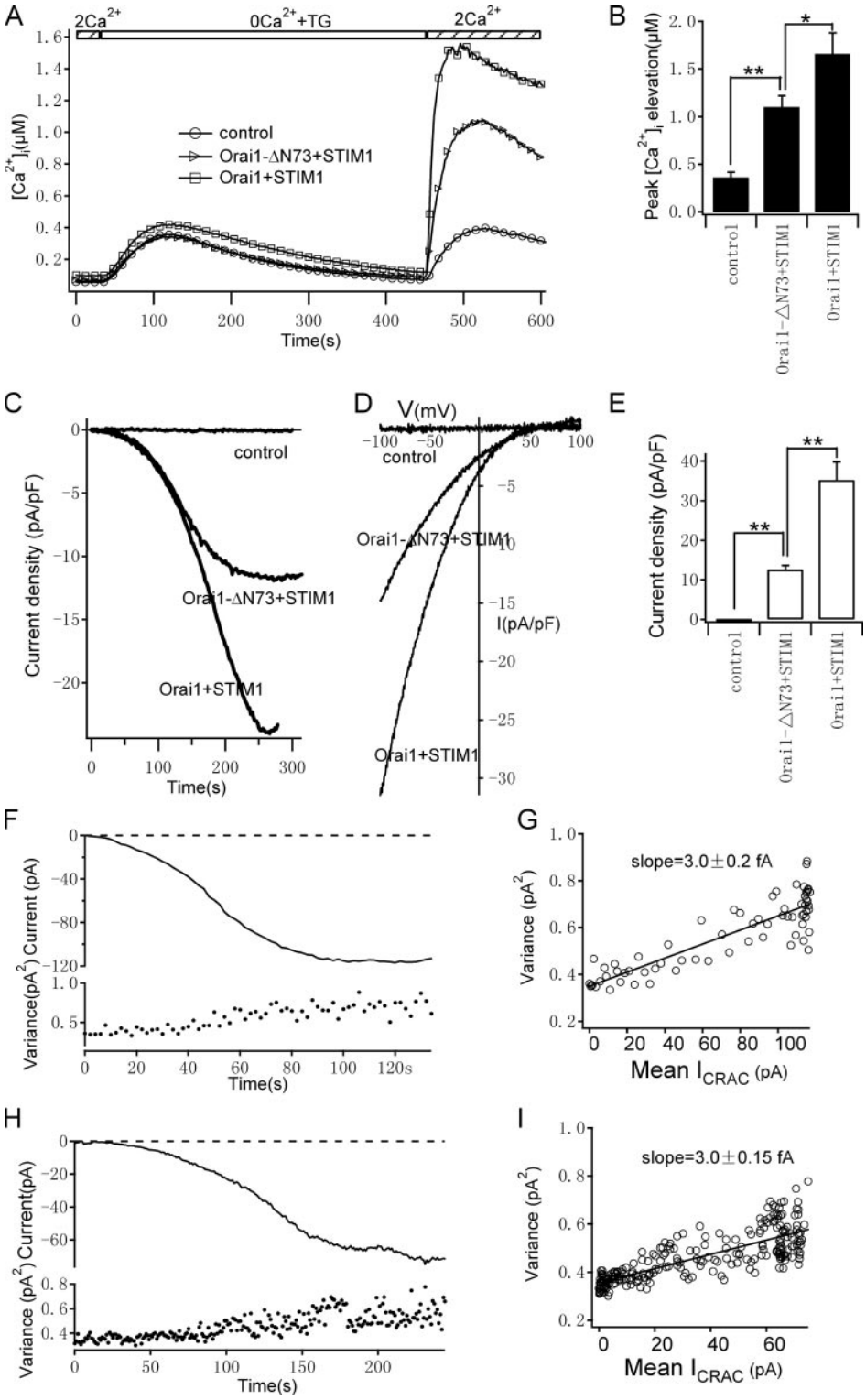


FIGURE 5. **Orai1 is capable of forming functional CRAC channels without amino acids 1–73 at the cytoplasmic N terminus.** *A*, HEK293 cells were co-transfected with Orai1-EGFP and STIM1-mOrange, Orai1-ΔN73, and STIM1-mOrange. Non-transfected cells were used as controls. Cells were pre-loaded with fura-2/AM and stimulated with TG (1 $\mu$M) in the $Ca^{2+}$-free solution to deplete the ER $Ca^{2+}$ store. Averaged time course of store depletion induced $Ca^{2+}$ entry in control HEK293 cells (circle, $n = 27$), cells expressed Orai1-ΔN73 and STIM1-mOrange (*right-facing triangle*, $n = 20$) and cells expressed Orai1-EGFP and STIM1-mOrange (*square*, $n = 22$). *B*, averaged peak $Ca^{2+}$ elevation in the indicated cells by re-addition of 2 mM $Ca^{2+}$ after store depletion. Significances of the *t* test are labeled on the histogram. *C*, representative time course of CRAC channel activation in cells as in *A*. No definitive CRAC current was detected in control cells, whereas substantial CRAC currents were observed in cells expressing fusion proteins. *D*, I-V curves at the time of maximal activation of the CRAC channel in *C*. *E*, summary of peak current densities at −100 mV in the indicated cell categories ($n = 8$ for each category); *p* values are labeled on the histogram. *F* and *H*, mean value and variance of CRAC current in cells co-expressing Orai1 plus STIM1 or Orai1-ΔN73 plus STIM1 after passive store depletion induced by dialysis of 12 mM BAPTA through the pipette. Each *point* represents the values calculated from a 200-ms segment of current data. *G* and *I*, the variances of CRAC current from *F* and *H* were plotted against mean currents and fitted with a linear function. The slope of the fit revealed the unitary single-channel CRAC currents at −100 mV in 10 mM extracellular $Ca^{2+}$ solution (see "Experimental Procedures").

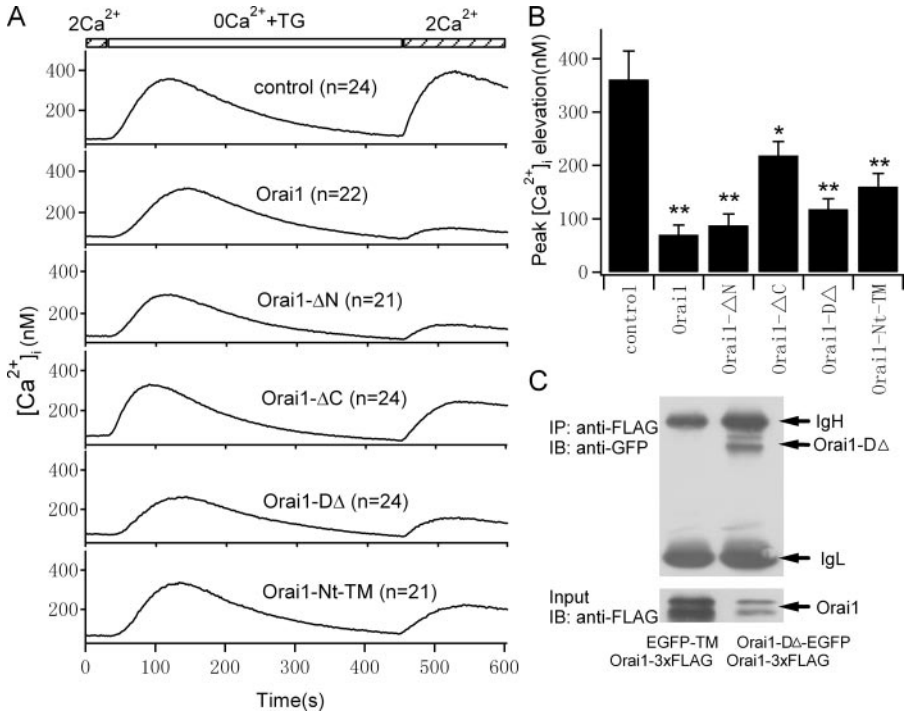


FIGURE 6. **Orai1 interact with each other using the transmembrane domain.** *A*, averaged SOC influx in HEK293 cells expressing WT Orai1-EGFP or Orai1 mutants after depletion of intracellular $Ca^{2+}$ store by TG. Non-transfected HEK293 cells were used as controls. Numbers of cells tested for each experiment are labeled on the figure. *B*, histograms of averaged peak $Ca^{2+}$ elevation of HEK293 cells in the indicated categories. * and **, statistical significance as compared with control. *C*, co-immunoprecipitation analysis of interaction between 3×FLAG-tagged WT Orai1 and EGFP-tagged Orai1-DΔ. EGFP-tagged transmembrane domain of Syx1A was used as a control. HEK293 cells were co-transfected with plasmids at a ratio of 1:1 encoding Orai1–3×FLAG and EGFP-TM or Orai1–3×FLAG and Orai1-DΔ-EGFP. Western blots of 3×FLAG-tagged wild-type Orai1 protein in whole cell lysate (*lower*) and EGFP-tagged Orai1-DΔ (*upper*) using the indicated antibodies.

polycationic tail is a vertebrate adaptation that helps STIM1 migration but not required for CRAC activation.

We also looked at functions of different domains of Orai1 in CRAC activation. It has recently been reported that the N terminus of murine Orai1 is essential for the store-operated $Ca^{2+}$ entry (23). In agreement with that report, we also found that truncation of the cytoplasmic N terminus of Orai1 failed to reconstitute SOC $Ca^{2+}$ entry when co-expressed with STIM1. Because there are five positively charged arginine residues in the N terminus of Orai1, it was postulated previously that these residues might bind to the ERM domain of STIM1 (23). However, truncation of the whole cytoplasmic N terminus did not affect store depletion-induced aggregation of Orai1 and its co-localization with STIM1, whereas deletion of the cytoplasmic C terminus diminished such responses. Conversely, overexpressing either Orai1-ΔN or Orai1-ΔC in HEK293 cells inhibited endogenous SOC $Ca^{2+}$ entry. This inhibition was reduced in cells co-expressing Orai1-ΔN and STIM1 but was not altered in cells co-expressing Orai1-ΔC and STIM1 (supplemental Fig. S7). Moreover, the plasma membrane-tethered N terminus of Orai1 did no co-localize with STIM1 clusters formed after store depletion (Fig. 4*C*). These three lines of evidence suggest that it is the cytoplasmic C terminus and not the N terminus of Orai1 that is crucial for the STIM1-Orai1 interaction. Rather, we believe that the N terminus of Orai1 is essential for the opening of CRAC channel. We identified a highly conserved region (amino acids 74–90) in the N terminus that is absolutely required for $I_{CRAC}$ activation. Because this region is conserved in human Orai1, Orai2, and Orai3, it may well explain the phenomenon wherein different Orai genes generate or augment store-operated $Ca^{2+}$ entry and reconstitute $I_{CRAC}$ current (25, 35–37). The reconstitute whole cell $I_{CRAC}$ current was smaller in cells co-expressing STIM1 and Orai1-ΔN73, compared with cells co-transfected with STIM1 and Orai1. Because the unitary single CRAC channel current revealed by the variance analysis of mean whole cell CRAC current was not altered (Fig. 5), the reduction in current could be due to a decreased open probability of single CRAC channel or an increase in the number of silent CRAC channels on the surface membrane (30). Whether any one of these hypotheses is true requires further investigation.

Orai1 forms dimers or oligomers in the non-stimulated resting state and store-depleted state (24, 25). Functionally overexpressing Orai1 in HEK293 and HeLa cells is found to inhibit endogenous SOC $Ca^{2+}$ entry (18, 35), implying that overexpressed Orai1 may interact with endogenous Orai1 and become insensitive to the store-depletion signal. In the present study, TG-induced endogenous SOC $Ca^{2+}$ entry was significantly inhibited in cells overexpressing Orai1-ΔC or Orai1-DΔ. Because Orai1-ΔC and -DΔ are deficient in their interaction with STIM1, the inhibition could only be due to interaction of endogenous Orai1 with these truncations. Moreover, co-immunoprecipitation experiments directly showed that Orai1-DΔ physically interacted with full-length Orai1. On the other hand, endogenous SOC $Ca^{2+}$ entry was inhibited by overexpressing Orai1-Nt-TM (Fig. 6, *A* and *B*), implying that the cytoplasmic N terminus may also participate in Orai1 oligomerization. Taking these findings together, we conclude that the transmembrane domain of Orai1 participates in Orai1 dimerization and oligomerization but does not exclude roles of other domains in the same processes.

In conclusion, after $Ca^{2+}$ store depletion, STIM1 aggregation requires the coiled-coil domain in the C terminus of STIM1. STIM1 migrates toward the surface membrane under guidance of both the serine-proline-rich region and the polycationic region, interacts with the cytoplasmic C terminus of Orai1, and leads to clustering of the latter on the opposing plasma membrane. Although the N terminus of the Orai1 is not required for its interaction with STIM1, amino acids 74–90 are essential for the opening of the CRAC channel. Finally, we propose that the transmembrane domain of Orai1 participates in Orai1-Orai1 interactions.

*Acknowledgment—We thank Prof. R. Y. Tsien for kindly providing mOrange cDNA.*

## REFERENCES


1. Berridge, M. J., Lipp, P., and Bootman, M. D. (2000) *Nat. Rev. Mol. Cell Biol.* **1,** 11–21
2. Parekh, A. B., and Putney, J. W., Jr. (2005) *Physiol. Rev.* **85,** 757–810
3. Takemura, H., and Putney, J. W., Jr. (1989) *Biochem. J.* **258,** 409–412
4. Putney, J. W., Jr. (1986) *Cell Calcium* **7,** 1–12
5. Hoth, M., and Penner, R. (1992) *Nature* **355,** 353–356
6. Roos, J., DiGregorio, P. J., Yeromin, A. V., Ohlsen, K., Lioudyno, M., Zhang, S., Safrina, O., Kozak, J. A., Wagner, S. L., Cahalan, M. D., Velicelebi, G., and Stauderman, K. A. (2005) *J. Cell Biol.* **169,** 435–445
7. Liou, J., Kim, M. L., Heo, W. D., Jones, J. T., Myers, J. W., Ferrell, J. E., Jr., and Meyer, T. (2005) *Curr. Biol.* **15,** 1235–1241
8. Feske, S., Gwack, Y., Prakriya, M., Srikanth, S., Puppel, S. H., Tanasa, B., Hogan, P. G., Lewis, R. S., Daly, M., and Rao, A. (2006) *Nature* **441,** 179–185
9. Vig, M., Peinelt, C., Beck, A., Koomoa, D. L., Rabah, D., Koblan-Huberson, M., Kraft, S., Turner, H., Fleig, A., Penner, R., and Kinet, J. P. (2006) *Science* **312,** 1220–1223
10. Zhang, S. L., Yeromin, A. V., Zhang, X. H., Yu, Y., Safrina, O., Penna, A., Roos, J., Stauderman, K. A., and Cahalan, M. D. (2006) *Proc. Natl. Acad. Sci. U. S. A.* **103,** 9357–9362
11. Stathopulos, P. B., Li, G. Y., Plevin, M. J., Ames, J. B., and Ikura, M. (2006) *J. Biol. Chem.* **281,** 35855–35862
12. Williams, R. T., Senior, P. V., Van Stekelenburg, L., Layton, J. E., Smith, P. J., and Dziadek, M. A. (2002) *Biochim. Biophys. Acta* **1596,** 131–137
13. Huang, G. N., Zeng, W., Kim, J. Y., Yuan, J. P., Han, L., Muallem, S., and Worley, P. F. (2006) *Nat. Cell Biol.* **8,** 1003–1010
14. Williams, R. T., Manji, S. S., Parker, N. J., Hancock, M. S., Van Stekelenburg, L., Eid, J. P., Senior, P. V., Kazenwadel, J. S., Shandala, T., Saint, R., Smith, P. J., and Dziadek, M. A. (2001) *Biochem. J.* **357,** 673–685
15. Draber, P., and Draberova, L. (2005) *Trends Immunol.* **26,** 621–624
16. Zhang, S. L., Yu, Y., Roos, J., Kozak, J. A., Deerinck, T. J., Ellisman, M. H., Stauderman, K. A., and Cahalan, M. D. (2005) *Nature* **437,** 902–905
17. Spassova, M. A., Soboloff, J., He, L. P., Xu, W., Dziadek, M. A., and Gill, D. L. (2006) *Proc. Natl. Acad. Sci. U. S. A.* **103,** 4040–4045
18. Soboloff, J., Spassova, M. A., Tang, X. D., Hewavitharana, T., Xu, W., and Gill, D. L. (2006) *J. Biol. Chem.* **281,** 20661–20665
19. Peinelt, C., Vig, M., Koomoa, D. L., Beck, A., Nadler, M. J., Koblan-Huberson, M., Lis, A., Fleig, A., Penner, R., and Kinet, J. P. (2006) *Nat. Cell Biol.* **8,** 771–773
20. Lorin-Nebel, C., Xing, J., Yan, X., and Strange, K. (2007) *J. Physiol.* **580,** 67–85
21. Xu, P., Lu, J., Li, Z., Yu, X., Chen, L., and Xu, T. (2006) *Biochem. Biophys. Res. Commun.* **350,** 969–976
22. Wu, M. M., Buchanan, J., Luik, R. M., and Lewis, R. S. (2006) *J. Cell Biol.* **174,** 803–813
23. Takahashi, Y., Murakami, M., Watanabe, H., Hasegawa, H., Ohba, T., Munehisa, Y., Nobori, K., Ono, K., Iijima, T., and Ito, H. (2007) *Biochem. Biophys. Res. Commun.* **356,** 45–52
24. Vig, M., Beck, A., Billingsley, J. M., Lis, A., Parvez, S., Peinelt, C., Koomoa, D. L., Soboloff, J., Gill, D. L., Fleig, A., Kinet, J. P., and Penner, R. (2006) *Curr. Biol.* **16,** 2073–2079
25. Gwack, Y., Srikanth, S., Feske, S., Cruz-Guilloty, F., Oh-Hora, M., Neems, D. S., Hogan, P. G., and Rao, A. (2007) *J. Biol. Chem.* **282,** 16232–16243
26. Yang, X., Xu, P., Xiao, Y., Xiong, X., and Xu, T. (2006) *J. Biol. Chem.* **281,** 15457–15463
27. Luik, R. M., Wu, M. M., Buchanan, J., and Lewis, R. S. (2006) *J. Cell. Biol.* **174,** 815–825
28. Chen, L., Koh, D. S., and Hille, B. (2003) *Diabetes* **52,** 1723–1731
29. Yeromin, A. V., Zhang, S. L., Jiang, W., Yu, Y., Safrina, O., and Cahalan, M. D. (2006) *Nature* **443,** 226–229
30. Prakriya, M., and Lewis, R. S. (2006) *J. Gen. Physiol.* **128,** 373–386
31. Baba, Y., Hayashi, K., Fujii, Y., Mizushima, A., Watarai, H., Wakamori, M., Numaga, T., Mori, Y., Iino, M., Hikida, M., and Kurosaki, T. (2006) *Proc. Natl. Acad. Sci. U. S. A.* **103,** 16704–16709
32. Heo, W. D., Inoue, T., Park, W. S., Kim, M. L., Park, B. O., Wandless, T. J., and Meyer, T. (2006) *Science* **314,** 1458–1461
33. Yeung, T., Terebiznik, M., Yu, L., Silvius, J., Abidi, W. M., Philips, M., Levine, T., Kapus, A., and Grinstein, S. (2006) *Science* **313,** 347–351
34. Liou, J., Fivaz, M., Inoue, T., and Meyer, T. (2007) *Proc. Natl. Acad. Sci. U. S. A.* **104,** 9301–9306
35. Mercer, J. C., Dehaven, W. I., Smyth, J. T., Wedel, B., Boyles, R. R., Bird, G. S., and Putney, J. W., Jr. (2006) *J. Biol. Chem.* **281,** 24979–24990
36. Dehaven, W. I., Smyth, J. T., Boyles, R. R., and Putney, J. W., Jr. (2007) *J. Biol. Chem.* **282,** 17548–17556
37. Lis, A., Peinelt, C., Beck, A., Parvez, S., Monteilh-Zoller, M., Fleig, A., and Penner, R. (2007) *Curr. Biol.* **17,** 794–800